Article

Not peer-reviewed version

Catalytic Pyrolysis of Açaí (*Euterpe oleracea* Mart.) Seeds: Circular Economy for Agro-industrial Waste-to-Energy in the Amazon

Douglas Alberto Rocha de Castro , Haroldo Jorge da Silva Ribeiro , Lauro Henrique Hamoy Guerreiro , Fernanda Paula da Costa Assunção , Lucas Pinto Bernar , Nilton Pereira da Silva , Daniela Muniz D'Antona Guimarães , Marta Chagas Monteiro , Luiz Eduardo Pizarro Borges , Kestin Kuchta , Nélio Teixeira Machado * , Sergio Duvoisin Junior

Posted Date: 24 March 2026

doi: 10.20944/preprints202603.1845.v1

Keywords: Açaí; residual seeds; pyrolysis; bio-oil; physicochemical properties; chemical composition; NaOH Impregnation

 doi:10.20944/preprints202603.1845.v1

Article

Catalytic Pyrolysis of Açaí (*Euterpe oleracea* Mart.) Seeds: Circular Economy for Agro-industrial Waste-to-Energy in the Amazon

Douglas Alberto Rocha de Castro [1,2], Haroldo Jorge da Silva Ribeiro [1], Lauro Henrique Hamoy Guerreiro [3], Fernanda Paula da Costa Assunção [3], Lucas Pinto Bernar [4], Nilton Pereira da Silva [5], Daniela Muniz D'Antona Guimarães [6], Marta Chagas Monteiro [7], Luiz Eduardo Pizarro Borges [8], Kestin Kuchta [9], Nélio Teixeira Machado [1,3,4,*] and Sergio Duvoisin Jr. [10]

[1] Graduate Program of Natural Resources Engineering of Amazon, Professional Campus-UFPA, Federal University of Pará, Rua Augusto Corrêa N° 1, Belém-PA 66075-110, Brazil
[2] Department of Chemical Engineering, Universidade Federal do Amazonas, Av. Gal. Rodrigo Octávio Jordão Ramos, 3000, Setor Norte, Coroado I, Manaus 69077-000, Brazil
[3] Graduate Program of Civil Engineering, Campus Profissional-UFPA, Universidade Federal do Pará, Rua Augusto Corrêa N° 1, Belém 66075-110, Brazil
[4] Faculty of Sanitary and Environmental Engineering, Campus Profissional-UFPA, Universidade Federal do Pará, Rua Augusto Corrêa N◦ 1, Belém 66075-900, Brazil
[5] Department of Mechanical Engineering, Federal University of Amazonas - UFAM, Av. General Rodrigo Octavio Jordão Ramos, 1200 - Coroado I, Manaus - AM, 69067-005, Brazil
[6] Department of Civil Engineering, Federal University of Amazonas- UFAM, Av. General Rodrigo Octavio Jordão Ramos, 1200 - Coroado I, Manaus - AM, 69067-005, Brazil
[7] Graduate Program of Pharmaceutical Sciences, Campus Profissional-UFPA, Universidade Federal do Pará, Rua Corrêa N◦ 1, Belém 66075-900, Brazil
[8] Laboratory of Catalyst Preparation and Catalytic Cracking, Section of Chemical Engineering, , Instituto Militar de Engenharia-IME, Praça General Tibúrcio N°. 80, Rio de Janeiro 22290-270, Brazil
[9] Institut für Circular Resource Engineering and Management – TUHH, Blohmstraße 15, 21079 Hamburg-Germany
[10] Department of Chemistry, Coordination of Chemical Engineering, Universidade do Estado do Amazonas-UEA, Avenida Darcy Vargas N°. 1200, Manaus 69050-020, Brazil
* Correspondence: author: machado@ufpa.br, Phone: +55-91-98462-0325

Abstract

In this study, the influence of chemical impregnation with an aqueous sodium hydroxide (NaOH) solution at 2 mol·L^{-1}, as well as process temperature, was systematically investigated at a pilot scale on the yield of pyrolysis products (bio-oil, gas, water, and biochar), as well as on the physicochemical properties (acid value, density, and kinematic viscosity) and chemical composition (hydrocarbons and oxygenated compounds) of the bio-oil obtained from açaí seeds (*Euterpe oleracea* Mart.). The pyrolysis reactions were carried out in a 143 L batch reactor at temperatures of 350 °C, 400 °C, and 450 °C under a pressure of 1.0 atmosphere. The NaOH impregnation played a crucial role in modifying the thermal degradation pathway of the biomass, promoting the formation of specific chemical structures and altering the product yields. NaOH acted as a catalyst, enhancing the deoxygenation of the biomass and stimulating the formation of hydrocarbons. As a result, the yields of bio-oil, water, biochar, and gas varied from 5.77 to 7.20% (by mass), 14.90 to 19.77% (by mass), 41 to 54% (by mass), and 25.33 to 32.03%, respectively, influenced by the increase in temperature. FT-IR analyses indicated the presence of characteristic chemical functions of hydrocarbons (alkanes, alkenes, and aromatics) and oxygenated compounds (phenols, cresols, ketones, esters, carboxylic acids, aldehydes, and furans), with an intensification of hydrocarbon signals at higher temperatures. GC-MS analysis confirmed hydrocarbons and oxygenated compounds as the main chemical classes in the bio-oil, showing a strong dependence on pyrolysis temperature. It was observed that the hydrocarbon concentration increased from 49.7% to 57.88% (area) with rising temperature, while the concentration of oxygenated compounds decreased from 13.88% to 6.69% (area), demonstrating that

 doi:10.20944/preprints202603.1845.v1

NaOH impregnation, combined with temperature elevation, favors the formation of hydrocarbons and the reduction of oxygenated compounds, thereby improving the quality of the produced bio-oil.

Keywords: Açaí; residual seeds; pyrolysis; bio-oil; physicochemical properties; chemical composition; NaOH Impregnation

1. Introduction

Açaí (Euterpe oleracea Mart.) is a native palm species naturally found in tropical regions of Central and South America [1], thriving in floodplains, swamps, and upland areas [2]. This palm produces dark-purple, berry-like fruits that grow in clusters [2]. Traditionally, the fresh fruits are processed by maceration or extraction of the pulp and skin using warm water, resulting in a thick, purple-colored beverage or paste [3,4]. Over time, açaí has become one of the most significant export commodities from the Amazon River estuary, both to other regions of Brazil [5] and internationally [6], accounting for 93.77% of total fruit, juice, and pulp exports between 2010 and 2016 [6].

The state of Pará is the largest national producer of açaí (Euterpe oleracea Mart.), with an annual production of 1,485,113 tons of fruit in the 2023 harvest year [6]. Of this total, approximately 83% to 85% by weight corresponds to processing residues, primarily açaí seeds [7,8], resulting in an estimated 1,232,643 to 1,262,346 tons/year of waste material. The metropolitan region of Belém, capital of the state of Pará (Brazil), comprises approximately 4,000 açaí-selling establishments [9], each processing, on average, between 4 and 10 boxes (14 kg per box) of fresh fruit daily, depending on the harvest season—August to January (crop season) and February to July (off-season) [10]. This results in the daily generation of approximately 190.4 tons of açaí seed residue during the off-season and 476.0 tons during the harvest season. Such volumes pose a significant solid waste management challenge for the metropolitan area of Belém and the surrounding municipalities.

The açaí (Euterpe oleracea Mart.) fruit is a small, dark purple, nearly spherical drupe, weighing between 2.6 and 3.0 g [11], with a diameter ranging from 10.0 to 20.0 mm [11]. It contains a large central seed, which accounts for approximately 85% of the fruit's total volume (vol./vol.) [3]. A fibrous layer is present between the seed (mesocarp) and the pericarp [11]. The seed itself is oily and fibrous, characterized by a high lignocellulosic content. Anatomically, the fruit is composed of an embryo, endocarp, scar, pulp, pericarp with tegument, and mesocarp [12].

The centesimal composition of açaí (Euterpe oleracea Mart.) fruit reveals a variable range of components, including lipids (1.65–3.56% wt.), total fiber (29.69–62.75% wt.), hemicellulose (9.01–14.19% wt.), cellulose (39.83–40.29% wt.), lignin (4.00–8.93% wt.), ash (0.15–1.68% wt.), moisture (10.15–39.39% wt.), and protein (5.02–7.85% wt.). Additionally, the fruit contains approximately 0.83% (wt.) fixed carbon and 7.82% (wt.) volatile matter [12–15].

In a global context where modern industrial society seeks to mitigate climate change, reduce CO_2 emissions, improve energy efficiency, and decrease dependence on fossil fuels, the adoption of renewable energy sources becomes imperative [16]. Within this framework, processes that reduce industrial and agro-industrial waste through reuse or recycling are essential, as they offer both environmental and energetic benefits to society [17]. Moreover, the recycling of such residues allows for the use of low-cost raw materials, thereby enhancing the economic feasibility of biofuel production [17].

Among the various renewable energy sources, biomass stands out as a promising alternative to conventional fossil fuels [18]. Its systematic use contributes to the mitigation of global warming when compared to fossil-based energy systems [19]. The carbon dioxide (CO_2) absorbed by plants during growth is subsequently released during combustion or decomposition of the biomass [18,19]. However, by replanting these crops, the newly growing vegetation can reabsorb the CO_2 emitted

 doi:10.20944/preprints202603.1845.v1

during processes such as carbonization (e.g., pyrolysis), thereby contributing to the closure of the carbon cycle, as noted by Kelli et al. [20].

A process that makes it possible the use of Açaí (Euterpe oleracea Mart.) seeds, a fiber residue, rich in lignin-cellulosic based material of low quality, for producing liquid bio-oils and gaseous fuels, and a solid phase adsorbent-like materials is pyrolysis, and the literature reports in the last years some studies on the pyrolysis of Açaí (Euterpe oleracea Mart.) seeds focusing on biofuels [15,21–29], including bio-oils physical-chemical properties [15,21,22,24–26,28], bio-oils chemical composition [15,21–23,25–28], distillation fractions physical-chemical properties [15,21,22], distillation fractions chemical composition [15,22], aqueous phase physical-chemical properties and chemical composition[25–28], as well as separation and/or purification processes to improve bio-oils quality [15,21,22].

Despite a few studies on the pyrolysis of Açaí (Euterpe oleracea Mart.) seeds focusing on biofuels using alkalis (KOH, NaOH) as catalysts [25,26,28], until the moment no study has been reported in the literature in real process systems, that is, in pilot scale, in order to investigated the influence of process temperature combined with chemical activation on the yields of pyrolysis products (bio-oil, gas, biochar, and aqueous phase), physicochemical properties and chemical composition of the produced bio-oils, as well as on the biochar properties. In this context, this study aims to investigate the influence of temperature combined with chemical activation (NaOH) on the yields pyrolysis products, physicochemical properties and chemical composition of bio-oils, as well as on the morphological and mineralogical characteristics of biochar, at 350, 400, and 450 °C, 1.0 atmospheric, in a pilot-scale system. The aim was to evaluate the real yield of pyrolysis products and to characterize the physicochemical properties and chemical composition of the produced bio-oil.

2. Materials and Methods

2.1. Materials

The açaí seeds (*Euterpe oleracea Mart*.) were naturally collected from a small commercial establishment selling açaí, located in the District of Guamá, Belém, Pará, Brazil. Figure 1 illustrates the anatomy of the açaí fruit in cross-section, highlighting the following structures: (1) embryo, (2) endocarp, (3) scar, (4) pulp, (5) pericarp with tegument, and (6) mesocarp [12].

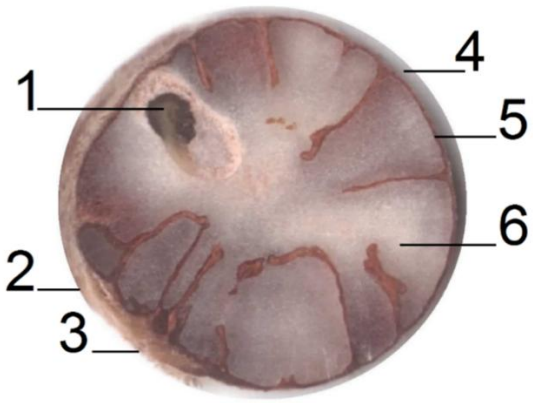

Figure 1. Anatomy of Açaí (Euterpe oleracea Mart.) fruit in nature (cross section): (1) embryo, (2) endocarp, (3) scar, (4) pulp, (5) pericarp + tegument, and (6) mesocarp.

2.2. Pre-Treatment of Açaí (Euterpe oleracea Mart.) Seeds and Chemical Impregnation Process

The seeds of Açaí were dried at 105°C using a pilot oven with air recirculation (SOC. FABBE. Ltda, Brazil, Model: 170) for a period of 24 hours. Afterward, the dried seeds were grinded using a laboratory knife cutting mill (TRAPP, Brazil, Model: TRF 600). Then, the dried and grinded Açaí seeds were sieved using an 18 Mesh sieve in order to remove the excess fiber material. A total of 14 charges of Açaí (Euterpe oleracea, Mart.) seeds in nature weighting approximately 10.0 kg were dried. At

 doi:10.20944/preprints202603.1845.v1

pilot scale, 32 kg of açaí seeds were impregnated with 64 L of 2.0 mol·L^{-1} aqueous NaOH solution (1:2 m/v ratio), using commercial caustic soda (UNIPAR CARBOCLORO, 95.5% purity). The process was carried out at the THERMITEK laboratory (UFPA) using a 110 L mechanical stirrer with a marine propeller, under ambient temperature, 1 atm, and 1000 RPM. After the impregnation period, the phases were separated by simple filtration using qualitative filter paper (Ø = 24 cm, 14 μm pore size). The solid phase was then dried at 100 ± 5 °C for 24 hours, preparing it for the slow pyrolysis process.

2.3. Characterization of Açaí Seeds Impregnated with Aqueous Sodium Hydroxide Solution

2.3.1. Thermogravimetric (TG/DTG) analysis of impregnated açaí (Euterpe oleracea, Mart) seeds

The thermal decomposition behavior of the impregnated açaí seeds was evaluated by thermogravimetric analysis (TG/DTG) using a Shimadzu thermal analyzer (Model DTG-60H, Japan). Approximately 5.0 mg of the sample was placed in a platinum crucible and subjected to a controlled heating program from 25 °C to 600 °C, at a constant heating rate of 10 °C min^{-1}, under a nitrogen atmosphere with a flow rate of 50 mL min^{-1}.

2.4. Pyrolysis Process of Impregnated Açaí Seeds on a Pilot Scale

The pyrolysis of açaí (Euterpe oleracea Mart.) seeds were carried out using an experimental apparatus like those described in the literature [21,29]. Liquid reaction products were collected every 20 minutes, recorded, and weighed. Subsequently, the samples underwent a decantation pretreatment to separate the aqueous and organic phases. The organic phase was then filtered to remove small solid particles.

2.5. Scanning Electron Microscopy and Energy Dispersive Spectroscopy (SEM/EDS)

Samples for SEM/EDS analysis were prepared by platinum (Pt) coating, forming a conductive film of 17.62 nm at a deposition rate of 0.09 nm/s under vacuum, using the Leica EM ACE600 high-vacuum coater. After metallization, samples were imaged using the FEI Quanta FEG250 SEM, at magnifications from 1000x to 5000x, with accelerating voltages of 15 kV and 20 kV, and image scales ranging from 100 μm to 20 μm. EDS analysis was performed using the QUANTAX EDS software and a BRUKER solid-state detector (EBSD) for elemental quantification.

2.6. X-Ray Powder Diffractometry (XRD)

The XRD characterization of the biochars was determined using an X-ray Diffractometer, model X'PERT PRO MPD (PW 3040/60) from PANalytical with the following specifications: CuK⊚ radiation, Ni filter, operating at 40 kV, 30 mA and wavelength λ = 0.154 nm and with X'Pert Data Collector software, (version 2.1a). The scanning interval was for 2θ values ranging from 5º to 75º. The scanning speed was 1º min-1 and the reading step was 0.01º. Thus, the influence of the impregnation process of the açaí seeds on the nature and crystalline structure of the chemical compositions of the biochars produced via pyrolysis was verified.

2.5. Physicochemical and Chemical Composition of Bio-Oils

2.5.1. Physicochemical Analysis of Bio-Oils and Distillation Fractions

Bio-oil physical-chemically characterized for acid value (AOCS Cd 3d-63), density (ASTM D4052) at 25°C, kinematic viscosity (ASTM D445/D446) at 40°C, and refractive index (AOCS Cc 7-25), as described in the literature [21,29,30]. The qualitative analysis of chemical functions (carboxylic acids, aliphatic and aromatic hydrocarbons, ketones, phenols, aldehydes, furans, esters, etc.) present in the bio-oil were performed by FT-IR spectroscopy according to the literature [21,29,31].

2.5.2. GC-MS of Bio-Oil

The separation and identification of all the compounds present in bio-oil were performed by CG-MS using a gas chromatograph (Agilent Technologies, USA, Model: CG-7890B), coupled to MS-5977A

 doi:10.20944/preprints202603.1845.v1

Mass Spectrometer, a SLBTM-5 ms (30 m × 0.25 mm × 0.25 mm) fused silica capillary column. The temperature conditions used in the CG-MS were injector temperature, 250°C; split, 1:50; detector temperature, 230°C; and quadrupole, 150 °C; injection volume, 1.0 ml; and oven, 60 °C/1 min, 3 °C/min, 200 °C/2 min, 20 °C/min, and 230 °C/10 min. The intensity, retention time, and compound identification were recorded for each peak analyzed according to the NIST (Standard Reference Database 1A, V14) mass spectra library which is part of the software. The identification is based on the similarity of the peak mass spectrum obtained with the spectra within the library database, included in the software [21]. The contents of all identified oxygenates and hydrocarbons present in each sample were separated, and the chemical composition of each experiment was estimated.

2.5.3. Fourier Transform Infrared Spectroscopy (FT-IR)

The infrared spectroscopy analysis was performed using a Shimadzu FTIR spectrophotometer, model IRAffinity-1S, equipped with an ATR8000 accessory. The spectra were obtained via horizontal attenuated total reflectance (ATR) using a ZnSe prism, with 64 scans and a resolution of 16.0 cm^{-1}. The spectra obtained from the biochar samples were compared with reference spectra from the substance database (library) available in the LabSolution Manager software. For the analysis, microparticles of the samples were applied to the infrared beam cavity of the ATR accessory, and the readings were performed using the LabSolutions IR software. The scanning range was from 400 to 4000 cm^{-1}.

3. Results and Discussions

3.1. Thermogravimetric (TG/DTG) Analysis of Impregnated Açaí (Euterpe oleracea, Mart) Seeds

The thermogravimetric analysis (TG/DTG) of açaí seeds impregnated with a 2 $mol \cdot L^{-1}$ aqueous NaOH solution, described in Figure 2, revealed three main thermal events. The first, occurring between 30 and 215 °C, corresponds to a continuous mass loss; up to 150 °C there is an approximate 8% reduction, attributed to moisture evaporation and the release of volatile compounds. This behavior is consistent with Bufalino et al. [32], who reported losses of up to 12% around 120 °C for in natura açaí seeds, and is further supported by Sait et al. [33], who associate this initial range with the removal of free and physically adsorbed water.

The second thermal event was subdivided into two intervals, 215–280 °C and 280–370 °C, totaling approximately 50% mass loss and attributed to the thermal degradation of hemicellulose and cellulose. The peaks observed in the DTG curve, particularly the more intense one around 250 °C and another near 300 °C, indicate simultaneous and secondary reactions, which align with the degradation ranges reported by Manara et al. [34], although their study presents single peaks for each component. The presence of two distinct peaks in the present work suggests structural alterations promoted by alkaline impregnation, possibly related to the cleavage of ester and ether linkages between lignin and carbohydrates, increasing the complexity of the thermal reactions.

The third event, observed between 370 and 600 °C, is associated with the degradation of lignin, the most recalcitrant fraction of the biomass. Unlike the behavior generally reported for açaí residues, where prominent peaks in this range are uncommon [34], the present study showed a more defined thermal event, indicating that the alkaline pretreatment may have modified the lignocellulosic structure and increased lignin susceptibility to thermal decomposition.

Complementary thermal analyses (DTA and DSC) support these interpretations. An endothermic event is observed below 100 °C, consistent with moisture removal. Between 190 and 600 °C, alternating endothermic and exothermic events occur, reflecting simultaneous degradation reactions of the organic matter and the inorganic fraction derived from the impregnated NaOH. Notably, there is an exothermic event between 190–225 °C and a significant endothermic peak between 225–280 °C, with an associated energy of 18.91 $J \cdot g^{-1}$ calculated by integrating the DSC curve.

In Castro's study [15] on in natura açaí seeds, typical thermal profiles of lignocellulosic biomasses are observed, with well-defined degradation temperatures for hemicellulose, cellulose,

 doi:10.20944/preprints202603.1845.v1

and lignin. When comparing these results with those of NaOH-impregnated seeds, a marked change in thermal kinetics is evident. The temperature associated with the highest mass-loss rate shifted from 305 °C to 250 °C, showing that the alkaline treatment reduced the thermal stability of the hemicellulosic fractions and anticipated the release of volatiles. This behavior suggests a catalytic effect, reflected in the reduction of characteristic temperatures normally observed in the pyrolysis of in natura lignocellulosic biomasses, implying greater formation of condensable and non-condensable gases at lower temperature ranges.

Thus, although the general degradation patterns (moisture, hemicellulose, cellulose, and lignin) remain consistent with the literature, the results demonstrate that alkaline impregnation with NaOH significantly altered the lignocellulosic structure of açaí seeds. This modification promoted the appearance of new peaks, greater overlap of thermal events, and a shift in characteristic degradation temperatures, reinforcing the potential of alkaline pretreatment to enhance biomass reactivity and justifying further studies aimed at its application in thermochemical processes for biofuel production.

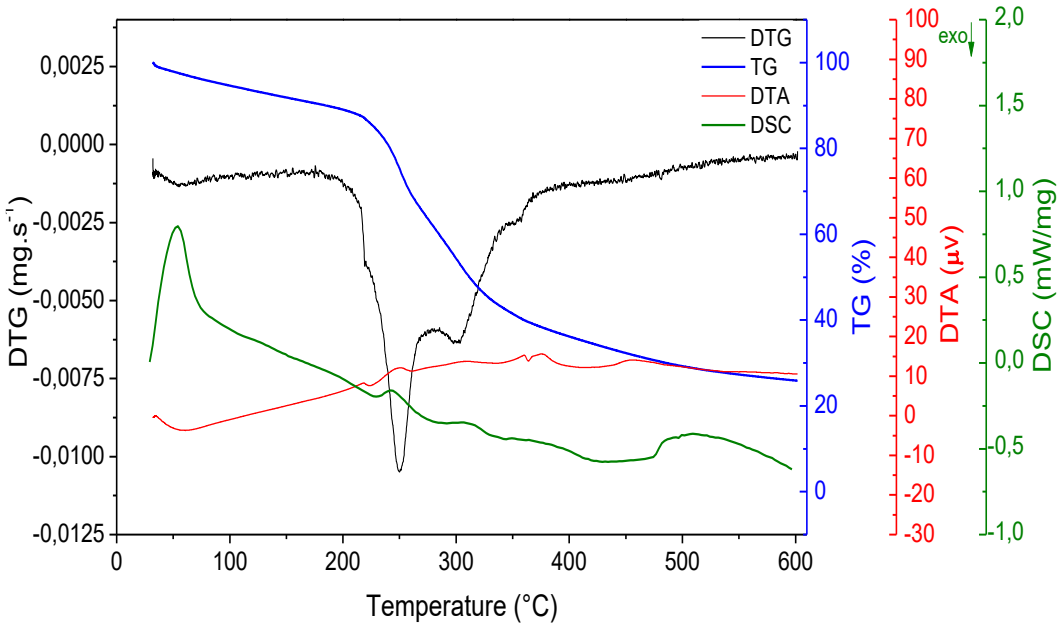

Figure 2. TG/DTG of impregnated açaí *(Euterpe oleracea, Mart)* seeds.

3.2. Pyrolysis Process Parameters of Impregnated Açaí (Euterpe oleracea Mart.) Seeds

The distribution of reaction products obtained from the slow pyrolysis of açaí seeds impregnated with 2.0 mol·L^{-1} NaOH, carried out at 350, 400, and 450 °C (Table 1 and Figure 3), highlights the thermochemical behavior of the chemically axtivated biomass. Alkaline (NaOH) axtivatiuon promotes the rupture of intermolecular bonds in the hemicellulose and cellulose chains and facilitates the cleavage of phenolic linkages in lignin, favoring thermal conversion and altering product yields.

Bio-oil yield decreases with the reduction in temperature (from 7.20% to 5.77%) due to the lower rate of thermal cracking and depolymerization, which limits the formation of condensable compounds. NaOH acts as a catalyst but also stimulates secondary reactions of recondensation and carbonization, reducing bio-oil yield. The aqueous fraction follows a similar trend (from 19.77% to 14.90%), consisting of reaction water and light oxygenated compounds, whose formation is intensified at higher temperatures due to thermal dehydration and condensation reactions.

The increase in biochar yield (from 41% to 54%) at lower temperatures agrees with the literature, as slow pyrolysis favors fixed-carbon retention and limits volatilization. The presence of NaOH contributes to the formation of more stable and porous carbonaceous structures, which are desirable for energetic or adsorption applications. The gaseous fraction (from 32.03% to 25.33%) increases with

 doi:10.20944/preprints202603.1845.v1

temperature, reflecting the intensification of cleavage reactions of C–C and C–O bonds in cellulose, hemicellulose, and lignin, resulting in the release of CO, CO_2, H_2, and CH_4.

These results are consistent with Valdez et al. [25], who observed, in the pyrolysis of açaí seeds activated with 2.0 M KOH at 350–450 °C, bio-oil yields ranging from 3.19 to 6.79%, aqueous fractions from 20.34 to 25.57%, biochar from 33.40 to 43.37%, and gases from 31.85 to 34.45%. They are also compatible with the findings of Serrão et al. [24] and Castro et al. [22], who reported bio-oil yields between 2.0 and 13.09% in different experimental scales. Similarly, the biochar yields obtained (27–72.5%) fall within the ranges described in other studies involving in natura and chemically activated açaí seeds [35–37].

Overall, the results corroborate the literature [38,39], which indicates that bio-oil yield tends to increase with temperature up to approximately 450 °C, reflecting the typical behavior of lignocellulosic biomass pyrolysis.

Table 1. Operational parameters of the pilot-scale pyrolysis process for NaOH-impregnated açaí seeds conducted at 350, 400, and 450 °C under atmospheric pressure.

Process Parameters	Temperature [°C]		
	450	400	350
Mass of Açaí (kg)	30	30	30
Mass of GLP (kg)	10.70	8.80	4.00
Cracking Time (min)	135	105	85
Time to reach Cracking Temperature (min)	105	75	55
Burning Time of the Gas Produced (min)	140	110	60
Initial Cracking Temperature (°C)	91	96	87
Mas of Aqueous Phase (Bio-oil and H_2O) (kg)	8.09	7.27	6.20
Mass of Biochar (kg)	12.30	14.30	16.20
Mass of Bio-oil (kg)	2.16	1.95	1.73
Mass of H_2O (kg)	5.93	5.32	4.47
Mass of Gas (kg)	9.61	8.43	7.60
Yield of Bio-oil (%)	7.20	6.50	5.77
Yield of Biochar (%)	41.0	47.67	54.0
Yield of H_2O (%)	19.77	17.73	14.90
Yield of Gas (%)	32.03	28.10	25.33

 doi:10.20944/preprints202603.1845.v1

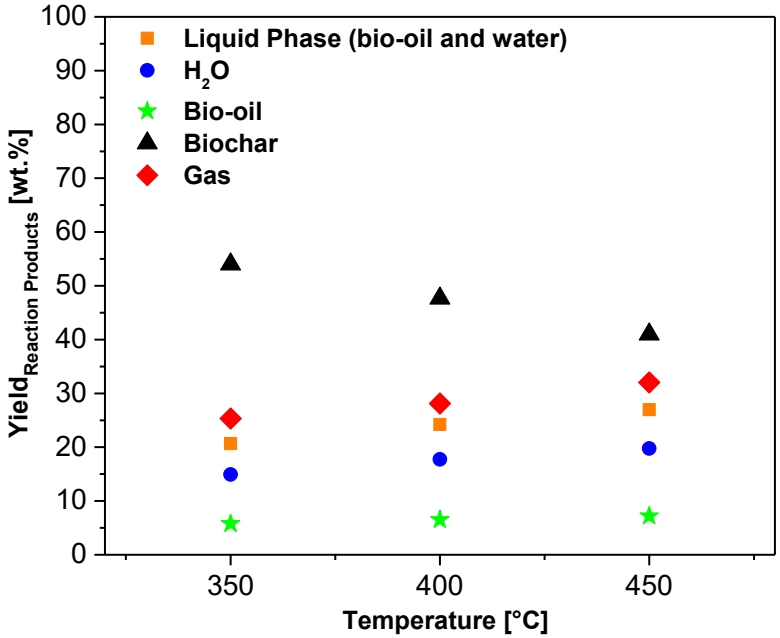

Figure 3. Yield of reaction products (bio-oil, H_2O, biochar, and gas) obtained from the pyrolysis of impregnated açaí *(Euterpe oleracea, Mart)* seeds at 350, 400, and 450 °C, 1.0 atmosphere, in semi-pilot scale.

3.3. Results of the Morphological, Crystallographic and Textural Characterization of the Biochars Produced

3.3.1. Scanning Electron Microscopy and Energy Dispersive Spectroscopy

The morphological analysis of the biochar's produced from açaí seeds impregnated with NaOH (Figure 4) reveals structural transformations directly influenced by the pyrolysis temperature and alkaline activation. This behavior can be compared to the observations of Costa et al. [40], Lima et al. [41], Mesquita et al. [42], and Miranda et al. [43], who investigated lignocellulosic materials under different processing conditions, highlighting changes induced by cutting, grinding, or chemical treatments.

In the studies by Costa et al. [40], the surface of ground lignocellulosic particles (8 and 14 Tyler) shows irregularities associated with the mechanical comminution process and particle friction. Although the origin of these irregularities is different mechanical rather than thermochemical there is a parallel with the biochar produced at 350 °C (Figure 4a), whose surface still preserves original features of the plant matrix, exhibiting irregular cavities and limited pore opening. As with the ground particles, the initial irregularity does not necessarily indicate high functional porosity but represents an early stage of structural modification.

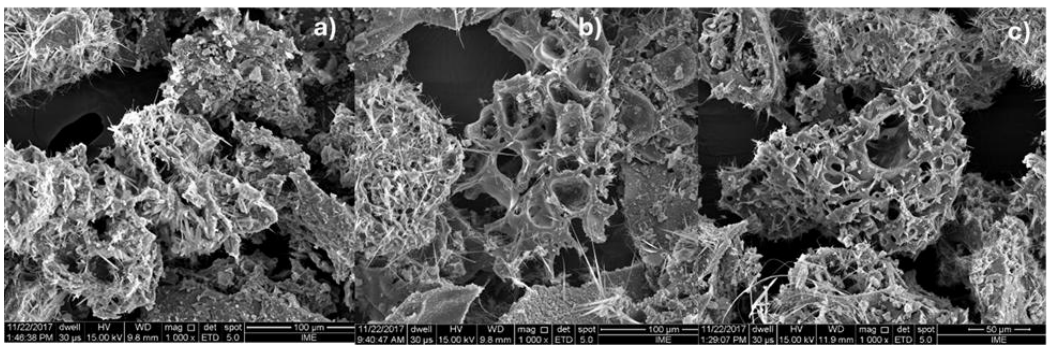

Figure 4. Micrographs of biochars impregnated with 2 M NaOH, produced at pyrolysis temperatures of 350°C (a), 400°C (b), and 450°C (c)., 1.0 atmosphere, in semi-pilot scale.

 doi:10.20944/preprints202603.1845.v1

Lima et al. [41] and Mesquita et al. [42] reported the presence of silica-rich protrusions on the surface of plant fibers, which provide greater mechanical rigidity and structural integrity. This contrasts with the behavior observed in the biochars produced at 400 °C and 450 °C (Figures 4b and 4c), in which alkaline activation promoted intense removal of organic matter and collapse of cell walls, resulting in more fragile, fragmented, and highly porous structures. Unlike the silica-enriched fibers where silica reinforces the matrix the NaOH impregnation induces selective degradation of hemicelluloses and cellulose, reducing structural strength and expanding the pore network.

Comparison with the chemical treatments described by Miranda et al. [43] reinforces this interpretation. These authors demonstrated that chemical agents capable of removing silica or other inorganic fractions can increase surface roughness and structural accessibility, provided they are applied with adequate intensity to avoid excessive defibrillation. Similarly, in the present study, increasing the pyrolysis temperature intensified the alkaline attack of NaOH, expanding pores and surface roughness. However, when the temperature reached 450 °C, degradation became more pronounced, producing a biochar with a highly open and fragmented morphology, characteristic of materials subjected to strong chemical activation.

Thus, whereas the works of Costa et al. [40] and Lima et al. [41] describe structural irregularities mainly resulting from mechanical processes or silica presence, the present study identifies that the combination of pyrolysis and alkaline impregnation leads to deeper modifications driven by thermochemical reactions. Likewise, studies such as that of Miranda et al. [115] indicate that chemical modification can enhance roughness and improve functional characteristics an effect also observed here, but with greater intensity due to the synergism between NaOH and temperature.

Overall, the results obtained for the NaOH-impregnated açaí seed biochars support the literature consensus that chemical activation and increasing temperature are key factors in the development of porosity and morphological heterogeneity. However, they differ from studies on non-carbonized plant fibers by showing that pyrolysis exponentially intensifies these effects, producing materials suitable for adsorption, catalysis, and energy applications.

Table 2 presents the EDS analysis results for the biochars produced at 350, 400, and 450 °C after impregnation with 2 M NaOH solution, allowing evaluation of how the elemental composition is modified by the temperature increase and the activating action of sodium hydroxide.

Table 2. EDS analysis for the of NaOH-impregnated açaí seed biochars, produced by *pyrolysis* at 350, 400, and 450 °C, 1.0 atmosphere, in semi-pilot scale.

Chemical Elements	Biochar 350 °C		Biochar 400 °C		Biochar 450 °C	
	Mass [wt%]	Atomic Mass [%]	Mass [wt%]	Atomic Mass [%]	Mass [wt%]	Atomic Mass [%]
C	43.73	54.86	50.50	61.12	64.14	74.58
O	31.59	29.75	28.82	26.17	17.64	15.42
Na	21.70	14.22	19.29	12.19	13.94	8.48
K	2.80	1.07	1.39	0.52	4.28	1.52
Mg	0.18	0.10	-	-	-	-
Total	100	100	100	100	100	100

The data reveals clear trends associated with progressive carbonization and the chemical evolution of the carbonaceous matrix. The carbon content (C) increases significantly with rising temperature, from 43.73 wt% in the biochar produced at 350 °C to 50.50 wt% at 400 °C, reaching 64.14 wt% at 450 °C. This behavior is typical of pyrolytic processes, in which volatile and oxygenated compounds are progressively removed, resulting in a matrix enriched in carbon. The increase in the relative atomic percentage of carbon, which reaches 74.58% at the highest temperature, indicates

 doi:10.20944/preprints202603.1845.v1

advancements in the degree of aromatization and carbonization features desirable for materials intended for adsorption, electrochemical applications, and energy systems.

Conversely, the oxygen (O) content decreases steadily with increasing temperature, from 31.59 wt% at 350 °C to 28.82 wt% at 400 °C and 17.64 wt% at 450 °C. This decline is associated with the removal of oxygen-containing functional groups through dehydration, decarboxylation, and decarbonylation, reactions characteristic of the pyrolysis process. The reduction in the atomic fraction of oxygen reinforces the formation of more stable and less polarized carbonaceous structures, directly influencing properties such as hydrophobicity and electrical conductivity.

The inorganic elements originating from alkaline impregnation show distinct behaviors. Sodium (Na), derived from NaOH, appears in high concentrations in all samples but decreases with increasing temperature, from 21.70 wt% to 19.29 wt% and then to 13.94 wt%. This trend suggests that part of the sodium is mobilized or volatilized at higher temperatures or becomes less superficially detectable due to carbon matrix reorganization. Nevertheless, the presence of Na in all samples confirms its strong interaction with the matrix and its role as an activating agent and mineral catalyst.

Potassium (K), although present at lower concentrations, exhibits a different trend: it decreases from 2.80 wt% to 1.39 wt% when the temperature increases from 350 to 400 °C, but rises to 4.28 wt% at 450 °C. This behavior may reflect both the heterogeneity of mineral distribution in the biomass and the greater exposure of mineral sites at elevated temperatures, when structural collapse releases elements previously encapsulated in the lignocellulosic matrix. The atomic fraction of K follows this variation, suggesting that potassium may become concentrated as volatile organic mass is removed at higher temperatures.

The residual presence of magnesium (Mg), only in the 350 °C sample indicates that this mineral likely to originating from the raw biomass is either removed or becomes undetectable at higher temperatures, possibly due to incorporation into phases less detectable by EDS or volatilization of its compounds.

Overall, the observed elemental evolution confirms the combined effect of pyrolysis and alkaline activation, with an increase in carbon content, gradual reduction of oxygen, and rearrangement of impregnated minerals. These patterns reinforce the enhanced degree of carbonization and suggest that the biochar produced at 450 °C exhibits more favorable chemical properties for applications requiring higher thermal stability, greater fixed carbon content, and higher carbon purity.

When comparing these results with the study by Cordeiro [44] on raw açaí seeds, a striking contrast is evident. Cordeiro describes a highly oxygenated surface, typical of untreated lignocellulosic materials, with low fixed carbon content and a strong presence of polar functional groups. In contrast, the biochar's produced in this study display carbon enrichment and a marked reduction in oxygen, revealing a significant transformation of the original biomass into a more aromatic, hydrophobic, and stable matrix. Thus, the comparison shows that alkaline treatment combined with pyrolysis intensifies the degree of carbonization relative to raw seeds, resulting in a material with properties more suitable for advanced applications such as adsorption, electrochemistry, and energy production.

3.3. X-Ray Diffractometry for Impregnated Biochars

The XRD analysis (Figure 5) of the biochar's impregnated with 2 M NaOH and produced at 350, 400, and 450 °C reveals important structural differences directly associated with the effect of alkaline impregnation and increasing pyrolysis temperature. The set of diffractograms confirms the presence of a predominantly amorphous matrix, a typical characteristic of biochar's, but with significant crystalline contributions resulting from the action of NaOH and the concentration of inorganic minerals.

 doi:10.20944/preprints202603.1845.v1

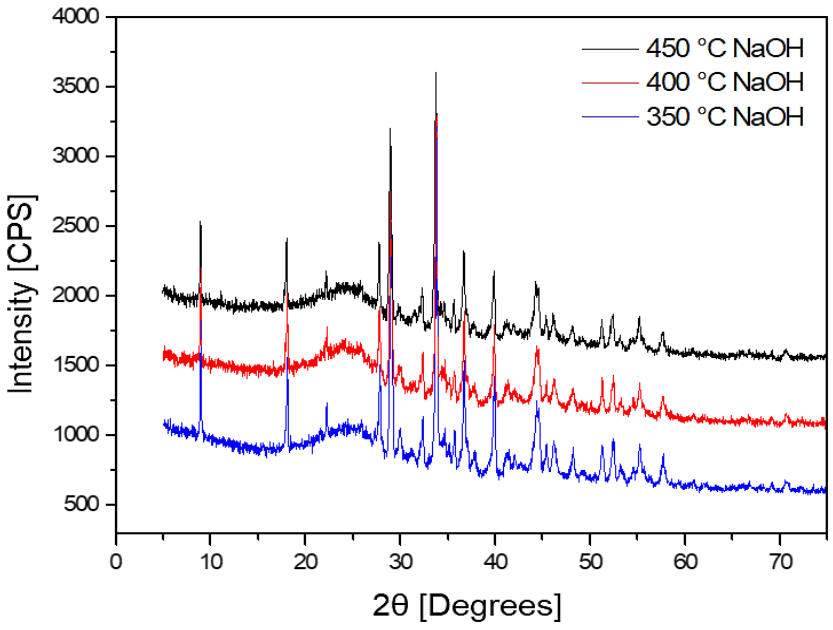

Figure 5. Micrographs and X-ray diffractograms of NaOH-impregnated açaí seed biochars, produced by *pyrolysis* at 350, 400, and 450 °C, 1.0 atmosphere, in semi-pilot scale, showing the formation of nanometric crystalline structures.

The XRD analysis of the biochars impregnated with 2 M NaOH and produced at 350, 400, and 450 °C shows a predominantly amorphous matrix, typical of lignocellulosic biochars, but with a marked presence of crystalline phases associated with the action of the alkaline activating agent and the pyrolysis temperature. The broad diffuse halo between 20–30° (2θ), related to turbostratic carbon structures, becomes more intense and defined as the temperature increases,particularly at 450 °C, indicating a higher degree of organization of graphitic domains and the onset of aromatization, a trend consistent with the increase in carbon content observed by EDS.

In addition to the amorphous fraction, the diffractograms reveal crystalline peaks whose intensity increases significantly in the samples treated at 400 and 450 °C, suggesting greater formation and stabilization of crystallized inorganic salts, including sodium and potassium carbonates and oxides. This behavior aligns with the findings of Prakongkep et al. [45], who identified Kalicinite ($KHCO_3$) as a dominant phase in chemically activated biochars, and Han Lee et al. [46], who reported similar patterns in materials modified with K-containing compounds. Complementarily, Díaz-Terán et al. [47] demonstrated that activation with KOH generates crystalline phases such as $KHCO_3$ and K_2CO_3, whose diffraction peaks increase in intensity with rising temperature, a phenomenon also observed in the samples of this study, particularly in those produced at 450 °C.

Thus, the results confirm that increasing the pyrolysis temperature intensifies both the structural organization of carbon and the crystallization of inorganic phases. The biochar produced at 450 °C exhibits the most defined diffractometric profile, indicating a higher degree of mineral reorganization and thermal maturation of the carbon matrix, consistent with patterns reported in the literature for chemically activated biochars. These findings reinforce that the combination of alkaline impregnation and elevated temperatures enhances the structuring of the biochar, increasing its thermal stability and its potential for applications that depend on higher crystallinity and greater availability of mineral active sites.

3.4. Physicochemical and Compositional Characterization of Bio-Oil

3.4.1. Density, Viscosity and Acid Value of Bio-Oil

The results obtained for the density of bio-oils generated by the pyrolysis of açaí seeds impregnated with 2 mol/L NaOH at temperatures of 450°C, 400°C and 350°C (Table 3) were,

 doi:10.20944/preprints202603.1845.v1

respectively, 1.02; 1.01 and 1.01 g/cm³. These values show little variation between them, indicating that the effect of temperature on density was not very significant within the range analyzed. However, it is possible to observe a slight tendency for density to increase with increasing temperature, which is in accordance with the literature, which reports that higher temperatures promote greater thermal degradation of biomass, favoring the formation of heavier compounds with lower oxygen content, which may contribute to an increase in bio-oil density.

Another relevant factor is the alkaline impregnation with NaOH, which can significantly influence the thermal degradation route of lignocellulosic biomass. NaOH acts by promoting saponification reactions and removal of acid and phenolic groups from lignin and hemicellulose, which can reduce the formation of oxygenated compounds and contribute to the production of more homogeneous liquid fractions, with lower relative density.

When compared with bio-oils obtained from other biomasses in the literature, the values observed (1.01–1.02 g/cm³) are within a range considered common for bio-oils from chemically treated lignocellulosic residues and are lower than those reported for raw agricultural residues such as rice or corn husks, which frequently have densities above 1.10 g/cm³. This difference can be attributed both to the chemical composition of the açaí seeds and to the action of NaOH, which can result in bio-oils with higher hydrocarbon content and lower oxygen and moisture content, characteristics that tend to reduce density. Therefore, the values obtained reflect a product with characteristics closer to light liquid fractions, which may be advantageous for certain energy applications, such as alternative liquid fuel, in addition to facilitating subsequent separation and refining processes.

The results obtained are close to the density of 1.06 g/mL (at 20°C) for bio-oil from softwood bark residues, as reported by Boucher *et al.* [48], and the density of 1.03 g/mL (at 20°C) for bio-oil from empty palm fruit bunches, as reported by Abnisa *et al.* [49]. However, they are lower than the density of 1.25 g/mL (at 20°C) for corn straw bio-oil reported by Yu *et al.* [50], and the density of 1.140 g/mL (at 30°C) for rice husk bio-oil according to Qiang *et al.* [51], at the density of 1.190 g/mL (at 20°C) for rice husk bio-oil according to Zheng and Wei [52], at the density of 1.1581 g/mL (at 20°C) for rice husk bio-oil according to Cai *et al.* [53], and at the density of 1.200 g/mL (at 20°C) for loblolly pine wood chip bio-oil reported by Tanneru *et al.* [54].

Table 3. Physicochemical characterization of bio-oil obtained from the pyrolysis of impregnated açaí (Euterpe oleracea, Mart) seeds at 450 °C, 400 °C, and 350 °C, 1.0 atmosphere, in semi-pilot scale.

Physicochemical Properties	450 °C	400 °C	350 °C	ANP Nº 65
	Bio-Oil	Bio-Oil	Bio-Oil	
ϱ [g/cm³], 30°C	1.02	1.01	1.01	0.82-0.85
I. A [(mg NaOH/g)]	19.44	19.91	20.71	-
I. R [-]	ND	ND	ND	-
⌀ [mm²/s], 40°C, *60°C	56.55	48.68	45.47	2.0-4.5

I.A = Acid Value; I.R = Refractive Index; ANP: Brazilian National Petroleum Agency, Resolution N° 65 (Specification of Diesel S10); ND = Not Determined.

The viscosity results of the bio-oils obtained by pyrolysis of açaí seeds impregnated with 2 molar NaOH indicate values of 56.55 mm²/s at 450°C, 48.68 mm²/s at 400°C and 45.47 mm²/s at 350°C. It is observed that the viscosity of bio-oils increased with increasing pyrolysis temperature, which is consistent with the formation of more complex and heavier organic compounds at higher temperatures. This behavior can be explained by the greater occurrence of secondary repolymerization and condensation reactions at higher temperatures, promoting the formation of heavier and more viscous fractions, such as polyaromatic phenols and high molecular weight

 doi:10.20944/preprints202603.1845.v1

compounds. Furthermore, the presence of NaOH may have catalyzed reactions that favor the formation of more complex and less volatile chemical structures. Comparing with the literature, the viscosity values obtained are within the range observed for bio-oils derived from lignocellulosic biomass, which generally vary between 20 and 100 mm²/s, depending on the type of raw material, pyrolysis conditions and residual water content. The lower viscosity observed at 350°C indicates a lighter bio-oil, with a higher proportion of volatile compounds, which may favor its application as a fuel or raw material for chemical refining. On the other hand, the higher viscosity at 450°C may require additional refining or dilution processes to enable its use in combustion or chemical processing systems.

These values are lower than the kinematic viscosity of 148 mm²/s at 60°C for corn stover bio-oil reported by Yu et al. [50], but higher than the viscosity of 38.0 mm²/s for softwood bark residues reported by Boucher et al. [48], 13.2 mm²/s for rice husk reported by Qiang et al. [51], 40.0 mm²/s (60°C) also for rice husk according to Zheng and Wei [52], values between 5.0–13.0 mm²/s (40°C) for rice husk reported by Cai et al. [53], and 12.0 mm²/s (40°C) for loblolly pine chips according to Tanneru et al. [154]. The kinematic viscosity results presented in Table 3 are in accordance with similar data found in the literature [48,50–54], which indicate that the kinematic viscosity of wood-derived bio-oils varies between 40 and 150 mm²/s, depending on the raw material, analysis temperature and pyrolysis conditions.

The results for the acidity index obtained for the bio-oils produced were 20.71 mg KOH/g, 19.91 mg KOH/g and 19.44 mg KOH/g, for the temperatures of 450°C, 400°C and 350°C, respectively. These results indicate a tendency for the acidity index to increase with the increase in the pyrolysis temperature, which may be associated with the greater thermal degradation of hemicellulose and cellulose, forming a greater amount of volatile organic acids in the bio-oil, especially acetic acid and substituted phenols, commonly present in pyrolysis products of lignocellulosic biomass.

Although the observed values are not as high as those reported for some biomasses that exceed 30 mg KOH/g, acidity values above 10 mg KOH/g still indicate high acidity, which may be problematic for storage, transportation and direct applications of bio-oil, especially as fuel, due to its corrosive potential and chemical instability. The impregnation with NaOH may have partially contributed to the neutralization of some acids formed, but the predominant effect of temperature seems to override this neutralization, since the increase in temperature favors cleavage reactions of C–O and C–C bonds in the biomass chains, generating more acidic oxygenated compounds.

3.4.2. Fourier Transform Infrared Spectrum

The infrared spectra (Figure 6) of the bio-oils obtained from the impregnated açaí seeds at pilot scale again show similarities in the identification of vibration bands (Table 4) with respect to the final temperatures investigated in the process. Small variations in the intensity (transmittance) of the main identified bands were also observed, with emphasis on the characteristic peaks of hydrocarbons (2960–2855 cm^{-1}), free amides (1685 cm^{-1}), and aromatic compounds (815–690 cm^{-1}). The FTIR spectroscopy results highlight a variety of functional groups present in the bio-oil produced from the pyrolysis of açaí seeds.

The absorption at 3360 cm^{-1}, associated with hydroxyl (–OH) groups, indicates the presence of compounds such as phenols and alcohols, suggesting that pyrolysis did not completely remove the oxygenated groups from the biomass. In addition, the peaks at 2960–2855 cm^{-1} and 1460 cm^{-1}, characteristic of aliphatic hydrocarbons (alkanes) and methylene groups ($–CH_2–$), indicate the formation of saturated aliphatic compounds such as alkanes during the pyrolysis process. These compounds are important for applications such as fuels.

The presence of oxygenated compounds is evidenced by the peaks at 1685 cm^{-1} (free amides), 1275–1020 cm^{-1} (esters, ethers, alcohols, and phenols), and 1110 cm^{-1} (secondary alcohol). These results suggest that, despite pyrolysis, there is significant formation of oxygenated compounds such as alcohols, esters, and phenols, derived from the degradation of lignocellulose. The peak at 1685 cm^{-1}

 doi:10.20944/preprints202603.1845.v1

also indicates the formation of amides, which may originate from proteins or nitrogen-containing compounds present in the biomass.

Finally, the peaks between 1595–1500 cm^{-1} and 815–690 cm^{-1}, associated with aromatic compounds, confirm the formation of aromatic rings such as benzene and its derivatives, which are typical products of lignocellulosic biomass pyrolysis. The presence of these aromatic compounds makes the bio-oil relevant for industrial applications, such as chemical intermediates and fuels.

The infrared spectra (Figure 6) of the bio-oils obtained from the impregnated açaí seeds at pilot scale again show similarities in the identification of vibration bands (Table 4) with respect to the final temperatures investigated in the process. Small variations in the intensity (transmittance) of the main identified bands were also observed, with emphasis on the characteristic peaks of hydrocarbons (2960–2855 cm^{-1}), free amides (1685 cm^{-1}), and aromatic compounds (815–690 cm^{-1}). The FTIR spectroscopy results highlight a variety of functional groups present in the bio-oil produced from the pyrolysis of açaí seeds.

Table 4. Functional Groups identified in bio-oils produced by pyrolysis of impregnated açaí (Euterpe oleracea, Mart) seeds at 450 °C, 400 °C, and 350 °C, 1.0 atmosphere, in semi-pilot scale.

Wavelength (cm^{-1})	Functional Groups	Bio-oil		
		350°C	400°C	450°C
3360	O – H hydroxyl (polymeric association)	X	X	X
2960-2855	Aliphatic C-H (Alkanes)	X	X	X
1685	C=O (free amides)	X	X	X
1595-1500	C=C (Aromatics)	X	X	X
1460	-CH_2- angular deformation (methylene groups)	X	X	X
1380	CH_3 angular deformation (dimethyl groups)	X	X	X
1275-1020	C-O (esters, ethers, alcohols and phenols)	X	X	X
1110	C-O (secondary alcohol)	X	X	X
815-690	C=C (aromatic rings 3H adj .)	X	X	X

The absorption at 3360 cm^{-1}, associated with hydroxyl (–OH) groups, indicates the presence of compounds such as phenols and alcohols, suggesting that pyrolysis did not completely remove the oxygenated groups from the biomass. In addition, the peaks at 2960–2855 cm^{-1} and 1460 cm^{-1}, characteristic of aliphatic hydrocarbons (alkanes) and methylene groups (–CH_2–), indicate the formation of saturated aliphatic compounds such as alkanes during the pyrolysis process. These compounds are important for applications such as fuels.

The presence of oxygenated compounds is evidenced by the peaks at 1685 cm^{-1} (free amides), 1275–1020 cm^{-1} (esters, ethers, alcohols, and phenols), and 1110 cm^{-1} (secondary alcohol). These results suggest that, despite pyrolysis, there is significant formation of oxygenated compounds such as alcohols, esters, and phenols, derived from the degradation of lignocellulose. The peak at 1685 cm^{-1} also indicates the formation of amides, which may originate from proteins or nitrogen-containing compounds present in the biomass. Thus, the pyrolysis of açaí seeds produces a complex bio-oil containing aliphatic and aromatic hydrocarbons, as well as oxygenated compounds. The observed behavior characterized by a complex mixture of hydrocarbons, aromatic compounds, and oxygenated species is consistent with results reported in previous studies [21–23,25–28,51,55–59], confirming that the bio-oil from açaí seeds has a composition similar to other bio-oils produced by slow or fast pyrolysis.

Accordingly, the FT-IR analysis confirms that, although pyrolysis promotes the generation of hydrocarbon fractions with potential for energy applications, the high concentration of oxygenated compounds indicates the need for additional upgrading steps, such as hydrotreatment,

 doi:10.20944/preprints202603.1845.v1

deoxygenation, or catalytic cracking if the goal is to obtain fuels with greater stability, lower acidity, and improved operational performance.

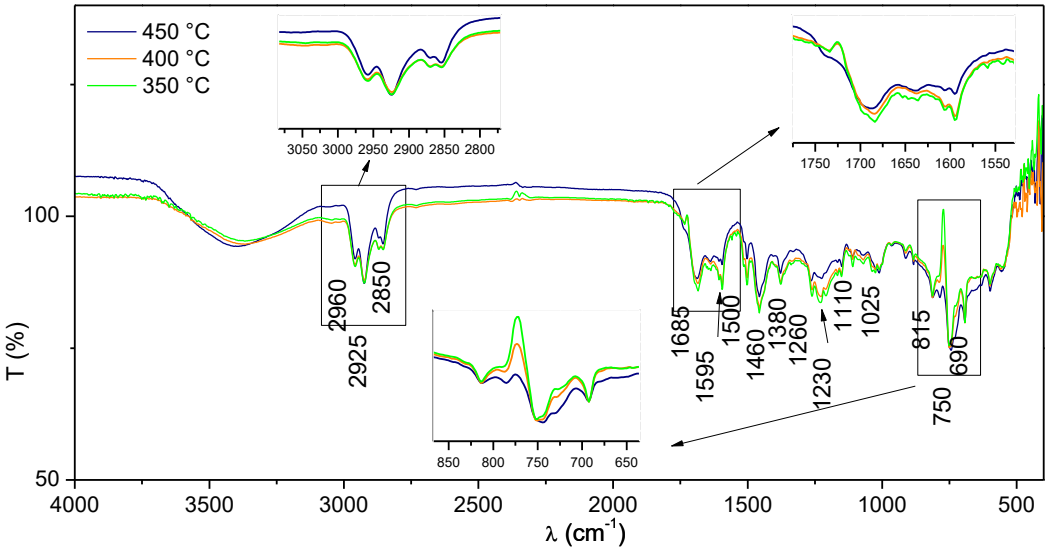

Figure 6. Infrared spectra of bio-oils produced by pyrolysis of impregnated açaí (Euterpe oleracea, Mart) seeds at 450 °C, 400 °C, and 350 °C, 1.0 atmosphere, in semi-pilot scale.

3.4.3. Gas Chromatography Coupled to Mass Spectrometry of Bio-Oils

The quantification of chemical compounds identified by GC-MS of bio-oils *produced* the pyrolysis of impregnated açaí (Euterpe oleracea, Mart) seeds at 450 °C, 400 °C, and 350 °C, 1.0 atmosphere, in semi-pilot scale is summarized in Table 5. The GC-MS of bio-oils produced by pyrolysis of açaí seeds impregnated with 2.0 mol·L^{-1} NaOH, at 450, 400, and 350 °C, 1.0 atmosphere, in semi-pilot scale, are shown in Tables 6–8 respectivelly. The bio-oils produced by pyrolysis of açaí seeds impregnated with NaOH indicate a predominance of hydrocarbons, with average values exceeding 20% for aromatic compounds and above 30% for aliphatic compounds, while nitrogenated and chlorinated species range between 3–15%. Naphthalene ($C_{10}H_8$) was the main compound identified under most conditions (≈11%), except at 450 °C, where Undecane ($C_{11}H_{24}$) became the major product (7.2%). The distribution of products varied with temperature: aromatics reached their maximum yield at 350 °C (32.6%) and subsequently decreased; aliphatics increased significantly from 400 °C onward (≈38–40%); and oxygenated compounds, initially low (≈6.7%), increased under more severe conditions, reaching up to 14%, indicating the secondary release of phenols, ketones, and related derivatives.

A comparison with alkaline pyrolysis using KOH as described elsewhere [26], reveals distinct trends. While NaOH maximizes aromatic formation at moderate temperatures, KOH promotes a continuous increase in these compounds with rising temperature, indicating a greater catalytic ability for aromatization under higher thermal regimes. Moreover, oxygenated compounds decrease exponentially in biomasses treated with KOH, a behavior described by first-order decay kinetic models (r^2 = 1.00), demonstrating the higher deoxygenation efficiency of potassium compared to sodium.

Table 5. Quantification of chemical compounds by GC-MS of bio-oils *produced* the pyrolysis of impregnated açaí (Euterpe oleracea, Mart) seeds at 450 °C, 400 °C, and 350 °C, 1.0 atmosphere, in semi-pilot scale.

Organic Groups	(% área)		
	350 [°C]	400 [°C]	450 [°C]

 doi:10.20944/preprints202603.1845.v1

Aromatic Hydrocarbons	32.611	16.998	19.804
Aliphatic Hydrocarbons	17.096	39.805	38.081
Ketones	9.264	-	3.618
Alcohol	4.924	5.955	11.738
Esters	1.452	2.278	1.441
Ethers	10.693	1.507	1.27
Aldehydes	9.425	3.462	5.582
Carboxylic Acid	1.453	2.097	2.019
Other Oxygenated	6.692	12.234	13.885
(Nitrogenated and Chlorinated)	6.387	15.665	2.563

Table 6. Classes of compounds, summation of peak areas, CAS number, and retention times of chemical compounds identified by CG-MS in bio-oil *produced* the pyrolysis of impregnated açaí (Euterpe oleracea, Mart) seeds at 450 °C, 1.0 atmosphere, in semi-pilot scale.

450°C			
Class of Compounds: Chemical Compounds	RT [min]	CAS	◎ᵢ% (Area)
Alkanes			
Undecane	10.622	1120-21-4	1.124
Tridecane	13.870	629-50-5	2.481
Pentadecane	16.744	629-62-9	2.290
Dodecane, 5,8-diethyl	19.326	24251-86-3	1.626
Σ (Area.%) =			**7.521**
Alkenes			
6-Tridecene, (Z)-	1.626	6508-77-6	2.118
***Σ (Area.%)* =**			**2.118**
Cycloalkenes			
Megastigma-4,6(E), 8 (Z)-trien	13.440	5298-13-5	1.847
***Σ (Area.%)* =**			**1.847**
Aromatic Hydrocarbons			
Naphthalene	12.262	91-20-3	4.399
Naphthalene, 1-methyl	14.046	90-12-0	2.390
1H-Indene, 1-ethylidene	14.296	2471-83-2	3.249
***Σ (Area.%)* =**			**10.038**
Esters			
Undecanoic acid, 10-methyl-, methyl ester	17.049	5129-56-6	1.096
Methyl tetradecanoate	19.620	124-10-7	2.969
***Σ (Area.%)* =**			**4.065**

 doi:10.20944/preprints202603.1845.v1

Carboxylic Acids			
Dodecanoic acid	17.648	334-48-5	4.307
Tetradecanoic acid	20.677	544-63-8	4.216
***Σ (Area.%)* =**			**8.523**
Ketones			
2-Pentanone, 4-hydroxy-4-methyl	5.886	123-42-2	1.878
2-Cyclopenten-1-one, 2,3-dimethyl	9.552	1121-05-7	1.655
***Σ (Area.%)* =**			**3.533**
Phenols			
Phenol	8.469	108-95-2	15.932
Phenol, 2-methoxy	10.446	90-05-1	4.583
Phenol, 2,6-dimethyl	10.805	576-26-1	1.991
Phenol, 2,4-dimethyl	11.469	105-67-9	2.034
Phenol, 2,5-dimethyl	11.502	95-87-4	2.215
Phenol, 3,4-dimethyl	11.821	95-65-8	3.845
Phenol, 4-ethyl-2-methoxy	13.571	2785-89-9	4.567
***Σ (Area.%)* =**			**35.167**
Cresols			
p-Cresol	9.818	108-39-4	6.331
m-Cresol	10.198	106-44-5	11.054
Cresol	12.210	93-51-3	3.141
***Σ (Area.%)* =**			**20.526**
Furans			
Benzofuran, 2-methyl	10.879	4265-26-2	1.879
Furan, 2-(2 furanylmethyl)-5-methyl	11.946	13678-51-8	2.089
Benzofuran, 4,7-dimethyl	12.700	28715-26-6	1.783
***Σ (Area.%)* =**			**5.751**
Aldehyds			
Cinnamaldehyde, β-methyl-	12.654	1196-67-4	0.910
***Σ (Area.%)* =**			**0.910**

Table 7. Classes of compounds, summation of peak areas, CAS number, and retention times of chemical compounds identified by CG-MS in bio-oil *produced* by pyrolysis of impregnated açaí (Euterpe oleracea, Mart) seeds at 400 °C, 1.0 atmosphere, in semi-pilot scale.

400°C			
Class of Compounds: Chemical Compounds	RT [min]	CAS	◎i% (Area)
Alkanes			
Tridecane	13.869	629-50-5	2.390

 doi:10.20944/preprints202603.1845.v1

Pentadecane	16.742	629-62-9	3.283
Σ (Area.%) =			**5.673**
Alkenes			
6-Tridecene, (Z)-	13.745	6508-77-6	2.553
7-Tetradecene	15.235	10373-74-0	1.231
Σ (Area.%) =			**3.784**
Cycloalkanes			
Cyclopentadecane	16.640	295-48-7	2.358
Σ (Area.%) =			**2.358**
Aromatic Hydrocarbons			
Naphthalene	12.260	91-20-3	4.002
Naphthalene, 1-methyl	14.045	90-12-0	2.282
1H-Indene, 1-ethylidene	14.295	2471-83-2	3.358
Σ (Area.%) =			**9.642**
Ketones			
2-Cyclopenten-1-one, 2,3-dimethyl	9.542	1121-05-7	2.100
Σ (Area.%) =			**2.100**
Phenols			
Phenol	8.468	108-95-2	27.049
Phenol, 2-methoxy	10.444	90-05-1	5.335
Phenol, 2,4-dimethyl	11.466	105-67-9	2.660
Phenol, 2,5-dimethyl	11.500	95-87-4	2.942
Phenol, 3,4-dimethyl	11.817	95-65-8	7.541
Phenol, 4-ethyl-2-methoxy	13.570	2785-89-9	4.827
Σ (Area.%) =			**50.354**
Cresols			
p-Cresol	9.815	108-39-4	7.844
m-Cresol	10.197	106-44-5	12.720
Cresol	12.208	93-51-3	3.957
Σ (Area.%) =			**24.521**
Furans			
Benzofuran, 4,7-dimethyl	12.697	28715-26-6	1.568
Σ (Area.%) =			**1.568**

Table 8. Classes of compounds, summation of peak areas, CAS number, and retention times of chemical compounds identified by CG-MS in bio-oil *produced* the pyrolysis of impregnated açaí (Euterpe oleracea, Mart) seeds at 450 °C, 1.0 atmosphere, in semi-pilot scale.

350°C

 doi:10.20944/preprints202603.1845.v1

Class of Compounds: Chemical Compounds	RT [min]	CAS	◎ᵢ% (Area)
Alkanes			
Tridecane	13.867	629-50-5	1.801
Pentadecane	16.741	629-62-9	1.855
Σ (Area.%) =			**3.656**
Alkenes			
6-Tridecene, (Z)-	13.744	6508-77-6	1.941
Σ (Area.%) =			**1.941**
Aromatic Hydrocarbons			
Naphthalene	12.258	91-20-3	3.037
Naphthalene, 1-methyl	14.043	90-12-0	1.887
1H-Indene, 1-ethylidene	14.294	2471-83-2	2.984
Σ (Area.%) =			**7.908**
Esters			
Undecanoic acid, 10-methyl-, methyl ester	17.046	5129-56-6	1.168
Methyl tetradecanoate	19.612	124-10-7	4.239
Σ (Area.%) =			**5.407**
Carboxylic Acids			
Dodecanoic acid	17.642	334-48-5	2.834
Σ (Area.%) =			**2.834**
Ketones			
2-Pentanone, 4-hydroxy-4-methyl	5.886	123-42-2	2.865
2-Cyclopenten-1-one, 2,3-dimethyl	9.552	1121-05-7	2.405
Σ (Area.%) =			**5.270**
Phenols			
Phenol	8.464	108-95-2	18.114
Phenol, 2-methoxy	10.442	90-05-1	6.342
Phenol, 2,6-dimethyl	10.802	576-26-1	1.654
Phenol, 2,4-dimethyl	11.465	105-67-9	2.422
Phenol, 2,5-dimethyl	11.499	95-87-4	2.680
Phenol, 2,3-dimethyl	11.783	526-75-0	2.936
Phenol, 3,4-dimethyl	11.816	95-65-8	4.141
Phenol, 4-ethyl-2-methoxy	13.567	2785-89-9	5.940
Phenol, 2-methoxy-4-propyl	14.914	2785-87-7	1.231
Σ (Area.%) =			**45.460**
Cresols			
p-Cresol	9.815	108-39-4	8.270
m-Cresol	10.195	106-44-5	11.547
Cresol	12.205	93-51-3	4.590

 doi:10.20944/preprints202603.1845.v1

Σ (Area.%) =			**24.407**
Furans			
Benzofuran, 4,7-dimethyl	12.697	28715-26-6	1.485
Benzofuran, 2-methyl	10.887	4265-26-2	1.632
Σ (Area.%) =			**3.117**

Sousa et al. [24] further corroborate this trend by showing that KOH markedly enhances the formation of alkanes, alkenes, and heterocyclic hydrocarbons, displaying an excellent exponential correlation ($r^2 = 1.00$). The authors also report a consistent decline in oxygenated compounds, which are preferentially transformed into hydrocarbons and light gases (CO, CO_2, and H_2O). According to their findings, KOH behaves as a highly reactive catalyst toward C–O and C–C bond cleavage, thereby intensifying aromatization and deoxygenation with increasing temperature.

Accordingly, the comparative analysis indicates that, although both NaOH and KOH promote hydrocarbon formation, NaOH tends to favor pathways marked by the predominance of aliphatic species and the re-emergence of oxygenated compounds under more severe conditions. In contrast, KOH as also demonstrated elsewhere [24], drives progressive aromatization, deeper deoxygenation, and a more efficient conversion of oxygenates into hydrocarbons. These distinctions underscore the specific catalytic role of each activating agent in steering the reaction pathway and in shaping the quality, stability, and energy potential of the resulting bio-oil.

4. Conclusions

In summary, the thermal analysis of NaOH-impregnated açaí seeds revealed moisture removal, sequential degradation of hemicellulose, cellulose, and lignin, as well as complex thermal events associated with the interaction of organic compounds and inorganic residues. The presence of multiple peaks in the DTG curve and the simultaneous exothermic and endothermic behavior highlight the influence of chemical treatment on modifying the thermal stability of the biomass.

The slow pyrolysis of NaOH-impregnated açaí seeds revealed that alkaline treatment strongly influences the distribution and yield of the resulting products. Higher temperatures promoted the formation of bio-oil and aqueous fractions due to the intensified thermal degradation and condensation of volatile compounds. At lower temperatures, a higher biochar yield was observed, associated with the preservation of fixed carbon and the development of porous and stable structures. The gas fraction increased with temperature, reflecting enhanced fragmentation of lignocellulosic chains. These findings highlight the role of NaOH as both a structural modifier and a catalyst in the thermochemical reactions of pyrolysis.

Overall, the chemical impregnation with NaOH markedly modified the morphology of the biochars, characterized by well-distributed porosity and the formation of sodium-based crystalline structures. The consistent elemental composition across the samples indicates that the chemical treatment conferred structural and compositional stability, regardless of the pyrolysis temperature.

Thus, it can be concluded that chemical impregnation with NaOH plays a decisive role in inducing crystallinity in the biochars by promoting the reorganization of the carbonaceous matrix at the nanometric scale. X-ray diffraction analysis confirms that the chemical treatment is primarily responsible for the formation of crystalline domains, while variations in pyrolysis temperature within the studied range (350–450 °C) have no significant impact on the final structure of the material. These findings highlight the importance of chemical pretreatment in engineering biochars with tailored structural properties for advanced applications.

The results demonstrate that alkaline impregnation with NaOH and pyrolysis temperature significantly influence the physicochemical properties of the bio-oils produced from açaí seeds. The density of the bio-oils remained practically constant, with a slight increasing trend at higher temperatures, indicating greater formation of heavier compounds. Viscosity increased proportionally

 doi:10.20944/preprints202603.1845.v1

with temperature, reflecting the generation of more complex and polymeric fractions at 450 °C. The acidity index also increased with temperature, suggesting higher production of volatile organic acids. Despite the observed variations, the values of density, viscosity, and acidity remained within the ranges reported for chemically treated lignocellulosic biomass bio-oils, highlighting the viability of the obtained bio-oil for energy applications, with potential additional treatments needed to reduce acidity and viscosity.

The analysis of the results from the pyrolysis of açaí seeds impregnated with 2 M NaOH reveals that temperature and alkaline impregnation significantly influence the formation of different compound groups in the bio-oil. The highest formation of aromatic hydrocarbons at 350 °C, followed by a decrease at higher temperatures, suggests that the alkaline environment promotes lignin depolymerization and the production of aromatic compounds under moderate thermal conditions. On the other hand, the formation of aliphatic hydrocarbons increased with temperature, especially from 400 °C onwards, indicating that NaOH plays a catalytic role in biomass cracking. The increasing production of oxygenated compounds, despite NaOH's deoxygenating action, reflects the release of such compounds as thermal degradation intensifies at higher temperatures. These results highlight the impact of temperature and NaOH treatment on the profile of compounds generated by pyrolysis, emphasizing the importance of controlling these variables to optimize the production of bio-oil with desirable characteristics for various applications.

Supplementary Materials: The following supporting information can be downloaded at: www.mdpi.com/xxx/s1, Table S1: Classes of compounds, summation of peak areas, CAS numbers, and retention times of chemical compounds identified by GC-MS in bio-oil obtained from the pyrolysis at 350 °C, 1.0 atm, of NaOH-impregnated açaí seeds at pilot scale. Table S2 Classes of compounds, summation of peak areas, CAS numbers, and retention times of chemical compounds identified by GC-MS in bio-oil obtained from the pyrolysis at 400 °C, 1.0 atm, of NaOH-impregnated açaí seeds at pilot scale. Table S3: Classes of compounds, summation of peak areas, CAS numbers, and retention times of chemical compounds identified by GC-MS in bio-oil obtained from the pyrolysis at 450 °C, 1.0 atm, of NaOH-impregnated açaí seeds at pilot scale.

Author Contributions: The individual contributions of all the co-authors are provided as follows: D.A.R.d.C. contributed with formal analysis and writing original draft preparation, investigation and methodology, H.J.d.S.R. contributed with formal analysis, investigation and methodology, L.H.R.G. contributed with investigation and methodology, F.P.d.C.A. contributed with investigation and methodology, L.P.B. contributed with investigation and methodology, N.P.S. contributed with resources and chemical analysis, D.A.G. contributed with resources and chemical analysis, M.C.M contributed with resources and chemical analysis, L.E.P.B. contributed with investigation, methodology and resources, K. K. contributed with process analysis, N.T.M contributed with draft preparation, investigation and supervision, S.D.Jr. contributed with chemical analysis and resources. All authors have read and agreed to the published version of the manuscript.

Funding: This research received no external funding.

Institutional Review Board Statement: Not applicable.

Informed Consent Statement: Not applicable.

Acknowledgments: I thank the Amazonas Research Foundation (FAPEAM) for the financial support provided, which was essential for the development of this project.

Conflicts of Interest: The authors declare no conflict of interest.

References

1. Jonny Everson Scherwinski-Pereira; Rodrigo da Silva Guedes; Ricardo Alexandre da Silva; Paulo César Poeta Fermino Jr.; Zanderluce Gomes Luis; Elínea de Oliveira Freitas. Somatic embryogenesis and plant regeneration in açaí palm (Euterpe oleracea). Plant Cell Tiss Organ Cult (2012) 109:501–508, DOI 10.1007/s11240-012-0115-z

 doi:10.20944/preprints202603.1845.v1

2. Alexander G. Schauss; Xianli Wu; Ronald L. Prior; Boxin Ou; Dinesh Patel; Dejian Huang; James P. Kababick. Phytochemical and Nutrient Composition of the Freeze-Dried Amazonian Palm Berry, Euterpe oleraceae Mart. (Acai). J. Agric. Food Chem. 2006, 54, 22, 8598-8603
3. Sara Sabbe; Wim Verbeke; Rosires Deliza; Virginia Matta; Patrick Van Damme. Effect of a health claim and personal characteristics on consumer acceptance of fruit juices with different concentrations of açaí (Euterpe oleracea Mart.). Appetite 53 (2009) 84–92, doi:10.1016/j.appet.2009.05.014
4. Lisbeth A. Pacheco-Palencia; Christopher E. Duncan; Stephen T. Talcott. Phytochemical composition and thermal stability of two commercial açai species, Euterpe oleracea and Euterpe precatoria. Food Chem. 115 (2009) 1199-1205, doi:10.1016/j.foodchem.2009.01.034
5. Eduardo S. Brondízio; Carolina A. M. Safar; Andréa D. Siqueira. The urban market of Açaí fruit (Euterpe oleracea Mart.) and rural land use change: Ethnographic insights into the role of price and land tenure constraining agricultural choices in the Amazon estuary. Urban Ecosystems (2002) 6-67, https://doi.org/10.1023/A:1025966613562
6. Corrêa, V. L. S., Ribeiro, H. J. D. S., Valois, F. P., Nascimento, M. Z. C. D., Silva, R. M. P., Martins, G. A. D. C., Ferreira, R. B. P., Brandão, I. W. D. S., Mendonça, N. M., & Machado, N. T. (2025). Statistical Analysis of Açaí Commercialization and Quantification of Waste Generated (Açaí Seeds) in the City of Belém/Pa. Preprints. https://doi.org/10.20944/preprints202502.2081.v1
7. Ana Victoria da Costa Almeida; Ingrid Moreira Melo; Isis Silva Pinheiro; Jessyca Farias Freitas; André Cristiano Silva Melo. Revalorização do caroço de açaí em uma beneficiadora de polpas do município de Ananindeua/PA: proposta de estruturação de um canal reverso orientado pela PNRS e logística reversa. GEPROS. Gestão da Produção, Operações e Sistemas, Bauru, Ano 12, Nº 3, jul-set/2017, 59-83. DOI: 10.15675/gepros.v12i3.1668
8. Claudio Ramalho Townsend; Newton de Lucena Costa; Ricardo Gomes de Araújo Pereira; Clóvis C. Diesel Senger. Características químico-bromatológica do caroço de açaí. COMUNICADO TÉCNICO Nº 193 (CT/193), EMBRAPA-CPAF Rondônia, ago./01, 1-5. ISSN 0103-9458, https://ainfo.cnptia.embrapa.br/digital/bitstream/item/100242/1/Cot193-acai.pdf
9. Carlos Fioravanti. Açaí: Do pé para o lanche. Revista Pesquisa Fapesp, Vol. 203, Janeiro de 2013, 64-68, http://revistapesquisa.fapesp.br/2013/01/11/folheie-a-edicao-203/
10. Antônio Cordeiro de Santana; Ádamo Lima de Santana; Ádina Lima de Santana; Marcos Antônio Souza dos Santos; Cyntia Meireles de Oliveira. Análise Discriminante Múltipla do Mercado Varejista de Açaí em Belém do Pará. Rev. Bras. Frutic., Jaboticabal - SP, Vol. 36, N°. 3, 532- 541, Setembro 2014, http://dx.doi.org/10.1590/0100-2945-362/13
11. José Dalton Cruz Pessoa; Paula Vanessa da Silva e Silva. Effect of temperature and storage on açaí (Euterpe oleracea) fruit water uptake: simulation of fruit transportation and pre-processing. Fruits, 2007, Vol. 62, 295–302; DOI: 10.1051/fruits:2007025 www.fruits-journal.org
12. Cordeiro M. A. Estudo da hidrólise enzimática do caroço de açaí (Euterpe oleracea, Mart) para a produção de etanol. Dissertação de Mestrado, Programa de Pós-Graduação em Engenharia Química, UFPA-Brazil. Marcio de Andrade Cordeiro; 2016
13. Tamiris Rio Branco da Fonseca; Taciana de Amorim Silva; Mircella Marialva Alecrim; Raimundo Felipe da Cruz Filho; Maria Francisca Simas Teixeira. Cultivation and nutritional studies of an edible mushroom from North Brazil. African Journal of Microbiology Research. 2015;9(30):1814-1822
14. Kababacknik A; Roger H. Determinação do poder calorífico do caroço do açaí em três distintas umidades, 38th Congresso Brasileiro de Química, São Luiz-MA-Brazil; 1998
15. CASTRO, Douglas Alberto Rocha de. *Processo de produção de bio-óleo e bio-adsorventes via pirólise das sementes de açaí (Euterpe oleracea Mart.)*. 2019. 300 f. Tese (Doutorado em Engenharia de Recursos Naturais) – Programa de Pós-Graduação em Engenharia de Recursos Naturais da Amazônia, Instituto de Tecnologia, Universidade Federal do Pará, Belém, 2019.
16. Michael Stöcker. Biofuels and Biomass-To-Liquid Fuels in the Biorefinery: Catalytic Conversion of Lignocellulosic Biomass using Porous Materials. Angew. Chem. Int. Ed. 2008, 47, 9200–9211

 doi:10.20944/preprints202603.1845.v1

17. Santos, A. L.F.; Martins, D. U.; Iha, O. K.; Ribeiro R. A.M.; Quirino R. L.; Suarez P. A.Z. Agro-industrial residues as low-price feedstock for diesel-like fuel production by thermal cracking. Bioresource Technology 101 (2010) 6157–6162
18. Diadem Özçimen; Ayşegül Ersoy-Meriçboyu. Characterization of biochar and bio-oil samples obtained from carbonization of various biomass materials. Renewable Energy, June 2010;35(6):1319-1324
19. David L. Nelson; Michael M. Cox: Leininger Principles of Biochemistry. 5th Edition. Freeman, New York, NY 2008, ISBN: 978-0-7167-7108-1
20. Kelli G. Roberts; Brent A. Glory; Stephen Joseph; Norman R. Scott; Johannes Lehmann. Life Cycle Assessment of Biochar Systems: Estimating the Energetic, Economic, and Climate Change Potential. Environ. Sci. Technol., 2010, 44 (2), 827–833
21. D. A. R. de Castroa; H. J. da Silva Ribeiro; C. C. Ferreira; L. H. H. Guerreiroa; M. de Andrade Cordeiro; A. M. Pereira; W. G. dos Santos; F. B. de Carvalho; J. O. C. Silva Jr.; R. Lopes e Oliveira; M. C. Santos; S. Duvoisin Jr; L. E. P. Borges; N. T. Machado. Fractional Distillation of Bio-Oil Produced by Pyrolysis of Açaí (Euterpe oleracea) Seeds. Editor Hassan Al-Haj Ibrahim: Fractionation, Intechopen ISBN: 978-1-78984-965-3, DOI: 10.5772/intechopen.79546
22. de Castro, D.R.; Ribeiro, H.D.S.; Guerreiro, L.H.; Bernar, L.P.; Bremer, S.J.; Santo, M.C.; Almeida, H.D.S.; Duvoisin, S.; Borges, L.P.; Machado, N.T. Production of Fuel-Like Fractions by Fractional Distillation of Bio-Oil from Açaí (Euterpe oleracea Mart.) Seeds Pyrolysis. Energies 2021, 14, 3713;
23. de Sousa,J.L.; Guerreiro, L.H.H.; Bernar, L.P.; Ribeiro, H.J.D.S.; e Oliveira, R.L.; Santos, M.C.; Almeida, H.D.S.; Junior, S.D.; Borges, L.E.P.; Castro, D.A.R.; et al. Chemical Analysis of Bio-Oil Produced by Pyrolysis of Açaí (Euterpe oleracea, Mart) Seeds. Braz. J. Dev. 2021, 7, 15549–15565.
24. Serrão, A.C.M.; Silva, C.M.S.; Assunção, F.P.D.C.; Ribeiro, H.J.D.S.; Santos, M.C.; Almeida, H.D.S.; Junior, S.D.; Borges, L.E.P.; de Castro, D.A.R.; Machado, N.T. Process analysis of pyrolysis of Açaí (Euterpe Oleracea, Mart) seeds: Influence of temperature on the yield of reaction products and physico-chemical properties of Bio-Oil. Braz. J. Dev. 2021, 7, 18200–18220
25. Daniel Valdez, G.; Valois, F.P.; Bremer, S.J.; Bezerra, K.C.A.; HamoyGuerreiro, L.H.; Santos, M.C.; Bernar, L.P.; Feio, W.P.; Moreira, L.G.S.; Mendonça, N.M.; et al. Improving the Bio-Oil Quality of Residual Biomass Pyrolysis by Chemical Activation: Effect of Alkalis and Acid Pre-Treatment. Energies 2023, 16, 3162. https://doi.org/ 10.3390/en16073162
26. Valois, F.P.; Bezerra, K.C.A.;Assunção, F.P.d.C.; Bernar, L.P.; daPaz, S.P.A.; Santos, M.C.; Feio, W.P.;Silva, R.M.P.; Mendonça, N.M.; deCastro, D.A.R.; et al. Improving theAntioxidant Activity, Yield, andHydrocarbon Content of Bio-Oil fromthe Pyrolysis of Açaí Seeds byChemical Activation: Effect ofTemperature and Molarity. Catalysts2024, 14, 44. https://doi.org/10.3390/catal14010044
27. Silva, I. C. d., Seabra, P. S. d. S., Lima, K. C. N., Filho, R. B. B., Santos, A. L. P. d., Monteiro, A. C. d. S., Pamplona, G. Q., da Silva Dias, A. G., Pereira, R. C. d. S., Costa, L. A., Pinheiro, T. J. M., Guerreiro, L. H. H., Machado, N. T., & Monteiro, M. C. (2025). Effect of Temperature and Molarity on the Evaluation of Antimicrobial, Cytotoxic, and Antioxidant Activities of the Bio-Oil from Açaí Seed (*Euterpe oleracea* Mart.). *International Journal of Molecular Sciences*, *26*(17), 8251. https://doi.org/10.3390/ijms26178251
28. de Sousa, E. M., Bezerra, K. C. A., Silva, R. M. P., Martins, G. A. d. C., de Assis, G. X., Ferreira, R. B. P., Bernar, L. P., Mendonça, N. M., Tavares Dias, C. G. B., Castro, D. A. R. d., Rodrigues, G. d. O., Junior, S. D., Monteiro, M. C., & Machado, N. T. (2025). Characterization of the Aqueous Phase from Pyrolysis of Açaí Seeds and Fibers (*Euterpe oleracea* Mart.). *Energies*, *18*(14), 3820. https://doi.org/10.3390/en18143820
29. da Mota S. A. P; Mâncio A. A; Lhamas D. E. L; de Abreu D. H; da Silva M. S; dos Santos W. G; de Castro D. A. R; de Oliveira R. M; Araújo M. E; Borges L. E. P; Machado N. T. Production of green diesel by thermal catalytic cracking of crude palm oil (Elaeis guineensis Jacq) in a pilot plant. Journal of Analytical and Applied Pyrolysis. 2014;110:1-11
30. Ferreira C. C; Costa E. C; de Castro D. A. R; Pereira M. S; Mâncio A. A; Santos M. C; Lhamas D. E. L; da Mota S. A. P; Leão A. C; Duvoisin S. Jr; Araújo M. E; Borges L. E. P; Machado N. T. Deacidification of organic liquid products by fractional distillation in laboratory and pilot scales. Journal of Analytical and Applied Pyrolysis. 2017;127:468-489

 doi:10.20944/preprints202603.1845.v1

31. Seshadri K. S; Cronauer D. C. Characterization of coal-derived liquids by 13C N.M.R. and FT-IR Spectroscopy. Fuel. 1983;62:1436-1444
32. Bufalino, L. , de Paula Protásio T. , Couto A. M. , Nassur O. A. C. , de Sá V. A. , Trugilho P. F. , and Mendes L. M. , "Chemical and energetic characterization for utilization of thinning and slab wood from Australian red cedar," Braz. J. For. Res. 32, 129–137 (2012).https://doi.org/10.4336/2012.pfb.70.13
33. Sait, H. H. , Hussain, A. , Salema, A. A. , and Ani, F. N. , "Pyrolysis and combustion kinetics of date palm biomass using thermogravimetric analysis," Bioresour. Technol. 118, 382–389 (2012).https://doi.org/10.1016/j.biortech.2012.04.081
34. Manara, P. , Zabaniotou, A. , Vanderghem, C. , and Richel, A. , "Lignin extraction from Mediterranean agro-wastes: Impact of pretreatment conditions on lignin chemical structure and thermal degradation behavior," Catal. Today 223, 25–34 (2014).https://doi.org/10.1016/j.cattod.2013.10.065
35. Guerreiro, L.H.H.; Baia, A.C.F.; Assunção, F.P.D.C.; Rodrigues, G.D.O.; e Oliveira, R.L.; Junior, S.D.; Pereira, A.M.; de Sousa, E.M.P.; Machado, N.T.; de Castro, D.A.R.; et al. Investigation of the Adsorption Process of Biochar Açaí (Euterpea olerácea Mart.) Seeds Produced by Pyrolysis. Energies 2022, 15, 6234.
36. Sato, M.K.; de Lima, H.V.; Costa, A.N.; Rodrigues, S.; Mooney, S.J.; Clarke, M.; Pedroso, A.J.; de Freitas Maia, C.M. Biochar as a sustainable alternative to ac¸ aí waste disposal in Amazon, Brazil. Process Saf. Environ. Prot. 2020, 139, 36–46
37. Zavarize, D.G. Insights on preparation and characteristics of KOH-doped carbons derived from an abundant agroindustrial waste in Brazil: Amazon açaí berry seeds. Bioresour. Technol. Rep. 2020, 13, 100611
38. Das, P.; Ganesh, A. Bio-oil from pyrolysis of cashew nutshell—A near fuel. Biomass Bioenergy 2003, 25, 113–117
39. Varma, A.K.; Mondal, P. Pyrolysis of sugarcane bagasse in semi batch reactor: Effects of process parameters on product yields and characterization of products. Ind. Crop. Prod. 2017, 95, 704–717
40. COSTA, R. G., ANDREOLA, K., MATTIETTO, R. A., et al., "Effect of operating conditions on the yield and quality of açaí (Euterpe oleracea Mart.) powder produced in spouted bed", LWT - Food Science and Technology, v.64, pp.1196-1203, Dez. 2015.
41. LIMA, A. M. de, CHRISTOFORO, A. L., FARIA, L. J. G., et al., "Influence of alkaline mercerization of treatment in the tensile strength of Açaí fiber", In: Non-conventional Building Materials based on agro industrial wastes, São Paulo, pp. 125-142, 2015.
42. MESQUITA, A. de L., Estudos de processos de extração e caracterização de fibras do fruto do Açaí (Euterpe oleracea MART.) da Amazônia para produção de ecopainel de partículas homogêneas de média densidade, 2013, 166 f., Tese de D.Sc, Universidade Federal do Pará, UFPA, Belém, PA, Brasil, 2013.
43. MIRANDA, C. S., FIUZA, R. P., CARVALHO, R. F., et al., "Efeito dos tratamentos superficiais nas propriedades do bagaço da fibra de piaçava (Attalea funifera Martius)", Química Nova, v. 38, n. 2, pp. 161 165, Nov. 2015.
44. CORDEIRO, M. A. Estudo da hidrólise enzimática do caroço de açaí (Euterpe oleraceae Mart.) para a produção de etanol. Dissertação de Mestrado. PPGEQ. Universidade Federal do Pará. 2016.
45. Prakongkep, N.; Gilkes, R.J.; Wiriyakitnateekul, W. Agronomic benefits of durian shell biochar. J. Met. Mater. Miner. 2014, 24, 7–11.
46. Lee, J.H.; Cha, Y.L.; Kang, Y.-M.; Roh, K.C. Study on the reaction mechanism of the potassium bicarbonate alkali activation process in black liquor. APL Mater. 2022, 10, 101105
47. Díaz-Terán, J.; Nevskaia, D.; Fierro, J.; López-Peinado, A.; Jerez, A. Study of chemical activation process of a lignocellulosic material with KOH by XPS and XRD. Microporous Mesoporous Mater. 2003, 60, 173–181
48. Boucher M. E; Chaala A; Roy C. Bio-oils obtained by vacuum pyrolysis of softwood bark as a liquid fuel for gas turbines. Part I: Properties of bio-oil and its blends with methanol and a pyrolytic aqueous phase. Biomass Bioenergy 2000;19:337–50
49. Abnisa F.; Arami-Niya A.; W. M. A. Wan Daud; J. N. Sahu. Characterization of bio-oil and bio-char from pyrolysis of palm oil wastes. Bioenergy Res 2013;6:830–40. http://dx.doi.org/10.1007/s12155-013-9313-8

 doi:10.20944/preprints202603.1845.v1

50. Fei Yu; Shaobo Deng; Paul Chen; Yuhuan Liu; Yiquin Wan; Andrew Olson; David Kittelson; Roger Rua. Physical and Chemical Properties of Bio-Oils From Microwave Pyrolysis of Corn Stover. Applied Biochemistry and Biotechnology 136–140 (2007) 957-970
51. Lu Qiang; Yang Xu-lai; ZhuXi-feng. Analysis on chemical and physical properties of bio-oil pyrolyzed from rice husk. Journal of Analytical and Applied Pyrolysis 82 (2008) 191-198
52. Ji-Lu Zheng; Qin Wei. Improving the quality of fast pyrolysis bio-oil by reduced pressure distillation. Biomass and Bioenergy 35 (2011) 1804-1810
53. Wenfei Cai; Ronghou Liu; Yifeng He; Meiyun Chai; Junmeng Cai. Bio-oil production from fast pyrolysis of rice husk in a commercial-scale plant with a downdraft circulating fluidized bed reactor. Fuel Processing Technology 171 (2018) 308-317
54. Sathish K. Tanneru; Divya R. Parapati; Philip H. Steele. Pretreatment of bio-oil followed by upgrading via esterification to boiler fuel. Energy 73 (2014) 214-220
55. Boateng A. A; Mullen C. A; Goldberg N; Hicks K. B. Production of bio-oil from alfalfa stems by fluidized-bed fast pyrolysis. Industrial and Engineering Chemistry Research. 2008;47:4115-4122
56. Xu Junming; Jiang Jianchun; SunYunjuan; LuYanju. Bio-Oil Upgrading by means of Ethyl Ester Production in Reactive Distillation to Remove Water to Improve Storage and Fuel Characteristics. Biomass and Bioenerg 32 (2008) 1056-1061
57. W.T.Tsaia; M. K. Lee; Y. M. Chang. Fast pyrolysis of rice husk: Product yields and compositions. Bioresource Technology, Volume 98, Issue 1, January 2007, 22-28
58. Elkasabi Y; Mullen C. A; Boateng A. A. Distillation and isolation of commodity chemicals from bio-oil made by tail-gas reactive pyrolysis. Sustainable. Chem. Eng. 2014;2:2042-2052
59. Rahul Garg; Neeru Anand; Dinesh Kumar. Pyrolysis of babool seeds (Acacia nilotica) in a fixed bed reactor and bio-oil characterization. Renewable Energy, Volume 96, Part A, October 2016, 167-171